Electronic Supplementary Material (ESI) for Journal of Materials Chemistry A.
This journal is © The Royal Society of Chemistry 2019

A novel *calendula*-like $MnNb_2O_6$ anchored on graphene sheet as high-performance intercalation pseudocapacitive anode for lithium-ion capacitors

Xu Zhang[a], Jinyu Zhang[a], Shuying Kong[b], Kai Zhu[a], Jun Yan[a] Ke Ye[a], Guiling Wang[a], Kui Cheng[a, c]**, Limin Zhou[c], Dianxue Cao[a]*

a. *Key Laboratory of Superlight Material and Surface Technology of Ministry of Education, College of Material Science and Chemical Engineering, Harbin Engineering University, Harbin 150001, China*

b. *Chongqing Key Laboratory of Special Functional Materials, Yangtze Normal University, Chong Qing 408100, China*

c. *Department of Mechanical Engineering, The Hong Kong Polytechnic University, Hung Hom, Kowloon, Hong Kong SAR, China*

Experimental

All the reagents were analytical grade and directly used after purchase without further purification.

Synthesis of 3D $MnNb_2O_6$@rGO

In a typical preparation, graphene oxide (GO) was prepared from natural graphite by a modified Hummers method[1, 2]. 0.1 g Nb_2O_5 was added into the KOH solution (0.2 mol L^{-1}, 30 mL) under constant stirring. Then transferring the mixture into a 100 mL Teflon-lined autoclave and heated to 220 °C for 24 h for transforming Nb_2O_5 into $[Nb_6O_{19}]^{8-}$.

---

* Corresponding author. E-mail address: chengkui@hrbeu.edu.cn (Kui Cheng), caodianxue@hrbeu.edu.cn (Dianxue Cao).

After cooling down naturally, using an appropriate amount of hydrochloric acid adjust the pH ≈ 9, and then 10 mL of $MnCl_2$ (in stoichiometric of Mn: Nb = 1: 2) and GO dispersion (0.1 mg mL^{-1}, 30 mL) were slowly added into above solution under continuous stirring. Transferring the mixed solution into a 100 mL Teflon-lined autoclave and heated to 220 °C for 48 h. Finally, the obtained $MnNb_2O_6$@rGO was washed repeatedly with ethanol and distilled water, and dried at 80℃ under a vacuum. Moreover, the $MnNb_2O_6$ was prepared following the procedures similar to that of $MnNb_2O_6$@rGO except the addition of GO solution for comparison.

Characterization

The morphology and structure of $MnNb_2O_6$@rGO, and $MnNb_2O_6$ were characterized by scanning electron microscope (SEM, JEOL JSM-6480) and transmission electron microscope (TEM, FEI Teccai G2S-Twin, Philips). The structure of the electrodes was characterized by an X-ray diffractometer (XRD, Rigaku TTR III) equipped with Cu-Kα radiation (λ = 0.1514178 nm) at a scan rate of 5° min^{-1}. Raman spectra were obtained on Renishaw InVia Reflex microscope with an excitation wavelength of 532 nm. The elemental analysis was performed with an elemental analyzer (Vario Micro cube). X-ray Photoelectron Spectroscopy (XPS) was carried out using a ThermoFisher ESCALAB™250Xi equipment to analyze the surface elemental composition of the materials. Thermogravimetric (TG) measurement was carried out to research the composition content of $MnNb_2O_6$@rGO using NETZSCH TG 209 F1 in air atmosphere from room temperature to 1000 °C at a heating rate of 10 °C min^{-1}.

Electrochemical measurements

For anode of LIC, a slurry containing 80 wt % $MnNb_2O_6$@rGO, 10 wt % Super P carbon black and 10 wt % polyvinylidene fluoride (PVDF) was well mixed, and then coated on a copper current collector and dried under vacuum at 80 ℃ for 24 h to remove the redundant methyl-2-pyrrolidone (NMP). Take out and cut it into rounds with the diameter of 14 mm. The cathode of LiC was prepared by coated with activated carbon (AC) on the Al foil similarly to the anode. The mass ratio of cathode to anode is 4:1. Finally, $MnNb_2O_6$@rGO cathode and AC anode were fabricated by employing coin type cells (2032), where we employed 1 M $LiPF_6$ dissolved in 1:1:1 by volume mixture of ethylene carbonate/diethyl carbonate/dimethyl carbonate (EC/DEC/EMC) as electrolyte, and separator (16 mm in diameter, celgard 2325).The fabrication of the half-cell is similar to that of the full cell (LIC), the only difference is to replace cathode material with Li metal foil.

All the electrochemical tests of LIC were carried out under the stable state after several CV cycles. Cyclic voltammetry (CV), galvanostatic charge/discharge (GCD) of as-prepared products were performed using a computerized potentiostat (Autolab PGSTAT302, Eco Chemie) controlled by GPES software. Long-term cycle life and rate performance of materails were performed employing a CT2001A cell test instrument (LAND Electronic Co., China). The specific capacitance (C, F g^{-1}) of $MnNb_2O_6$@rGO//AC full cell can be calculated according to the following formula:[3]

$$C = \frac{\Delta t}{m \times \Delta V^2} \int_{V1}^{V2} I dV \qquad (1)$$

The energy density (*E*, Wh kg^{-1}) and power density (*P*, W kg^{-1}) were calculated according to the following equations:[4, 5]

$$E = \frac{1}{2 \times 3.6} C V^2 \tag{2}$$

$$P = \frac{E}{\Delta t} \times 1000 \tag{3}$$

Where I (mA) and $\varDelta t$ (s) represent the discharge current and total discharge time. m (mg) and $\varDelta V$ (V) are assigned as the mass of active material and the potential window, respectively.

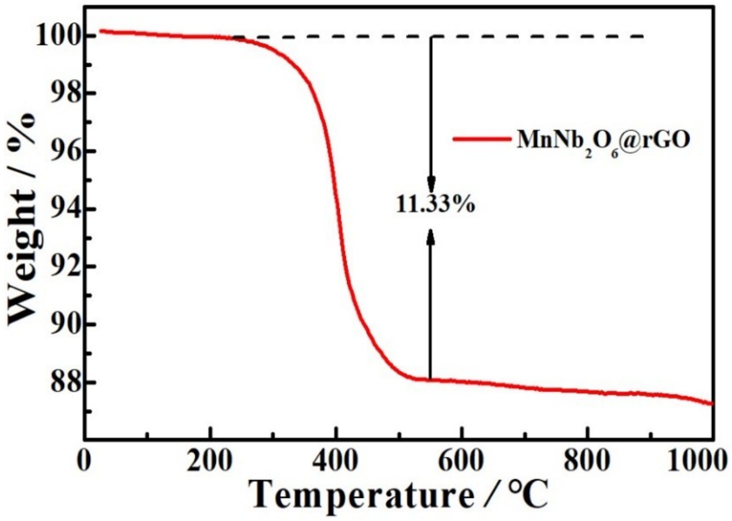

Figure S1 TG curves of the $MnNb_2O_6$@rGO

Table S1 The atomic ratio of $MnNb_2O_6$@rGO before and after Ar ion sputtering

Etching depth	5 nm	13 nm	21 nm
O1s	50.16	44.78	40.17
Nb3d	15.96	14.04	11.12
Mn2p	7.83	7.12	5.55
C1s	26.05	34.06	43.16

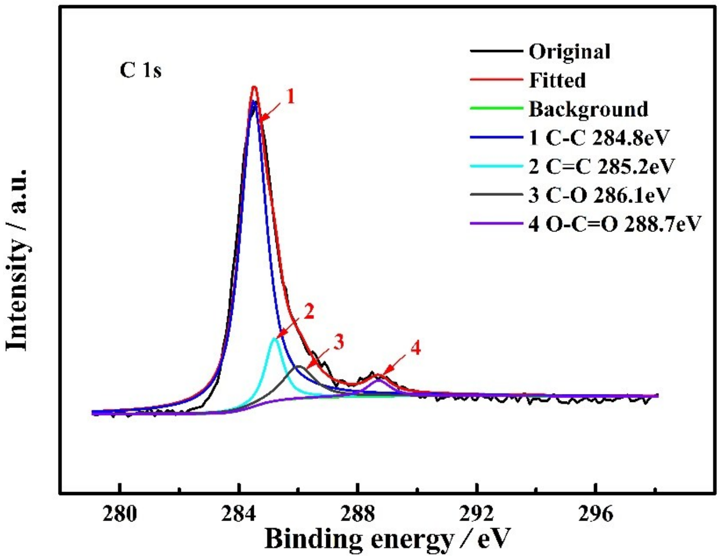

Figure S2 C$_{1s}$ XPS spectra of $MnNb_2O_6$@rGO

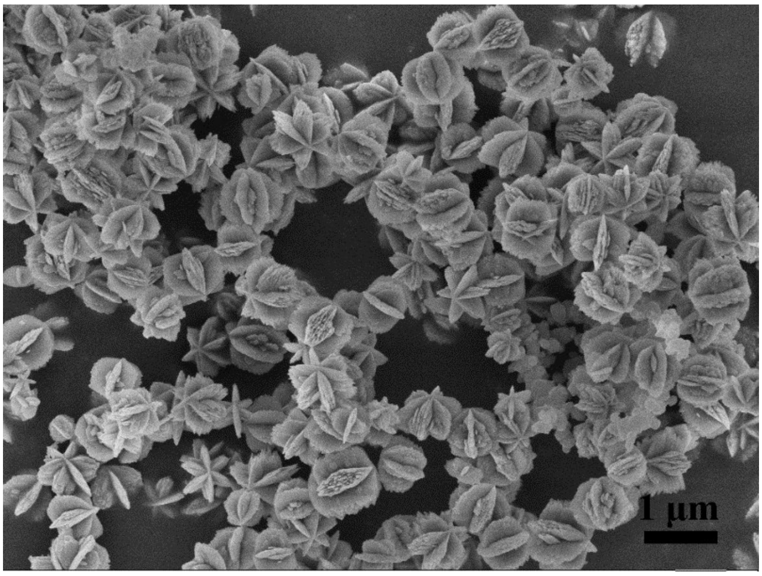

Figure S3 SEM images of $MnNb_2O_6$

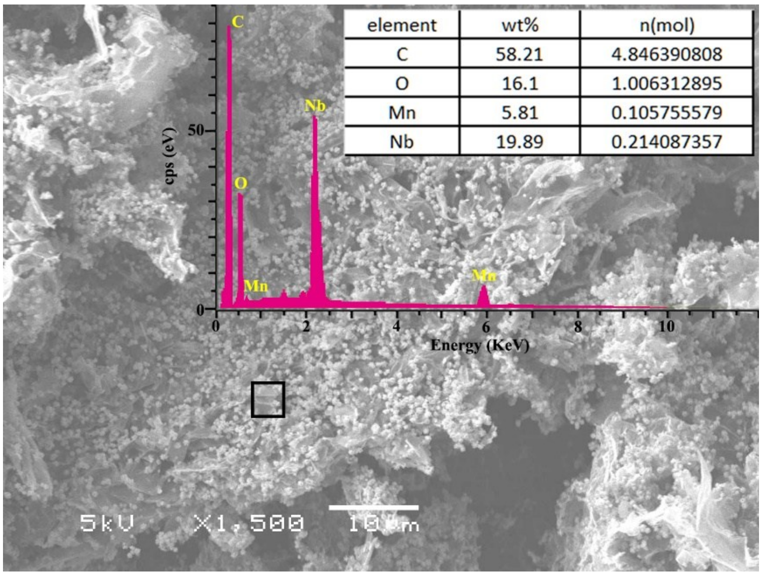

element	wt%	n(mol)
C	58.21	4.846390808
O	16.1	1.006312895
Mn	5.81	0.105755579
Nb	19.89	0.214087357

Figure S4 The EDS pattern of $MnNb_2O_6$@rGO

Table S2. The Li-ion storage capacity of $MnNb_2O_6$@rGO compared with other intercalation-type anode materials reported in the literature.

Anode	Li-ion storage capacity	Ref.
Li_3VO_4/N-Doped Carbon Nanowires	400 mAh g^{-1} at 100 mA g^{-1}	6
3D Interconnected TiC Nanoparticle Chains	450 mAh g^{-1} at 100 mA g^{-1}	7
$Li_4Ti_5O_{12}$/graphene composite	212.9 mAh g^{-1} at 0.5C 158.9 mAh g^{-1} at 20C	8
Nano-sized hierarchical $Li_{3.5}Ti_5O_{12}$	190 mAh g^{-1} at 0.5C 170 mAh g^{-1} at 50C	9
Co/LTO core/shell arrays	174 mAh g^{-1} at 1C	10

	155 mAh g^{-1} at 20C	
Walnut-like Porous Core/Shell TiO_2	176.7 mAh g^{-1} at 1C 126.4 mAh g^{-1} at 20C	11
Mesoporous H-Nb_2O_5/rGO	190 mAh g^{-1} at 100 mA g^{-1} 150 mAh g^{-1} at 1000 mA g^{-1}	12
$Mg_2Nb_{34}O_{87}$ Porous Microspheres	338 mAh g^{-1} at 0.1C 230 mAh g^{-1} at 10C	13
$MnNb_2O_6$@rGO calendula	460 mAh g^{-1} at 50 mA g^{-1} 200 mAh g^{-1} at 2000 mA g^{-1}	This work

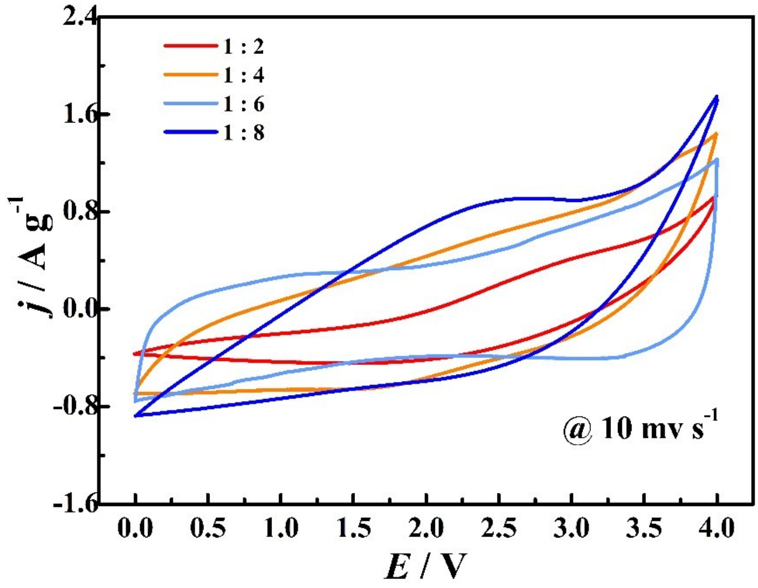

Figure S5 The CV curves of different anode/cathode weight ratios (1:2, 1:4, 1:6, 1:8)

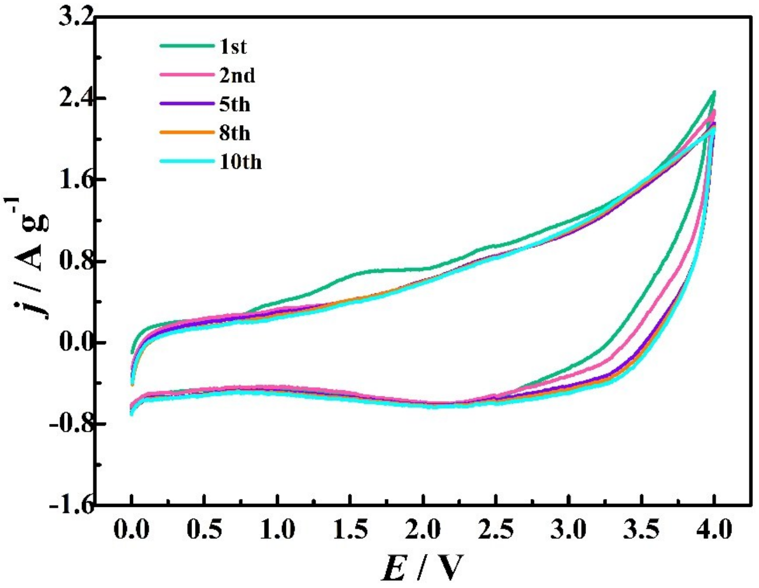

Figure S6 First 10 cycles for CV curves of the assembled device

A distinct bulge can be observed in 1st cycle during charging process, due to the formation of SEI layers in the lithium intercalation process.

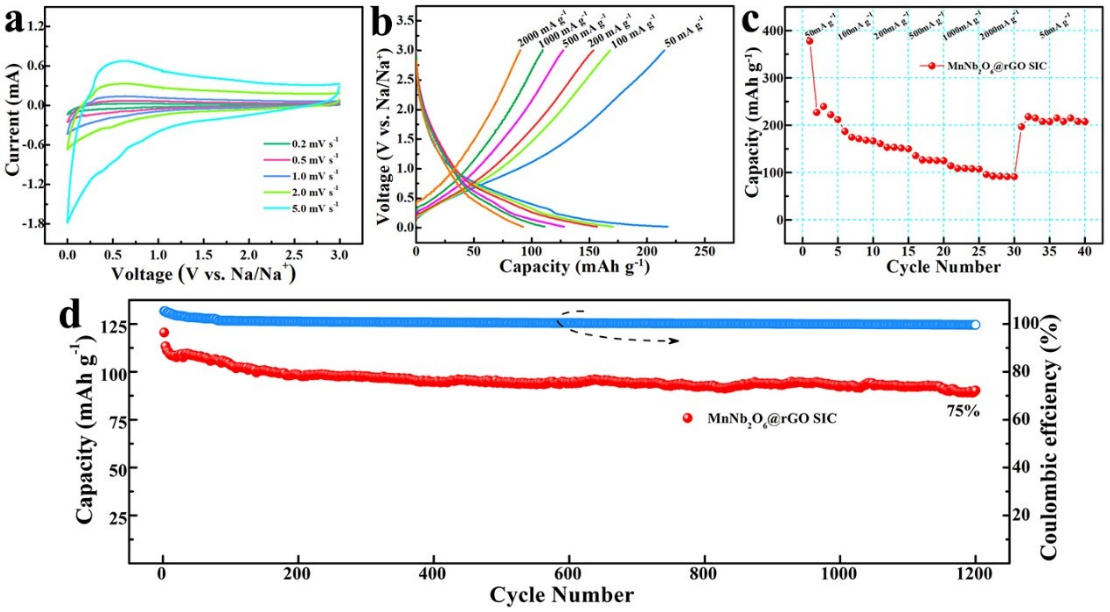

Figure S7. Na-ion storage performance of $MnNb_2O_6$@rGO. **(a)** CV curves at various scan rates from 0.2 to 5 mV s^{-1}; **(b)** Charge/Discharge curves at varied current densities from 50 to 2000 mA g^{-1}; **(c)** Rate performance at various current densities from 50 to 2000 mA g^{-1}; **(d)** The long-term cycle life and the coulombic efficiency at 500 mA g^{-1}.

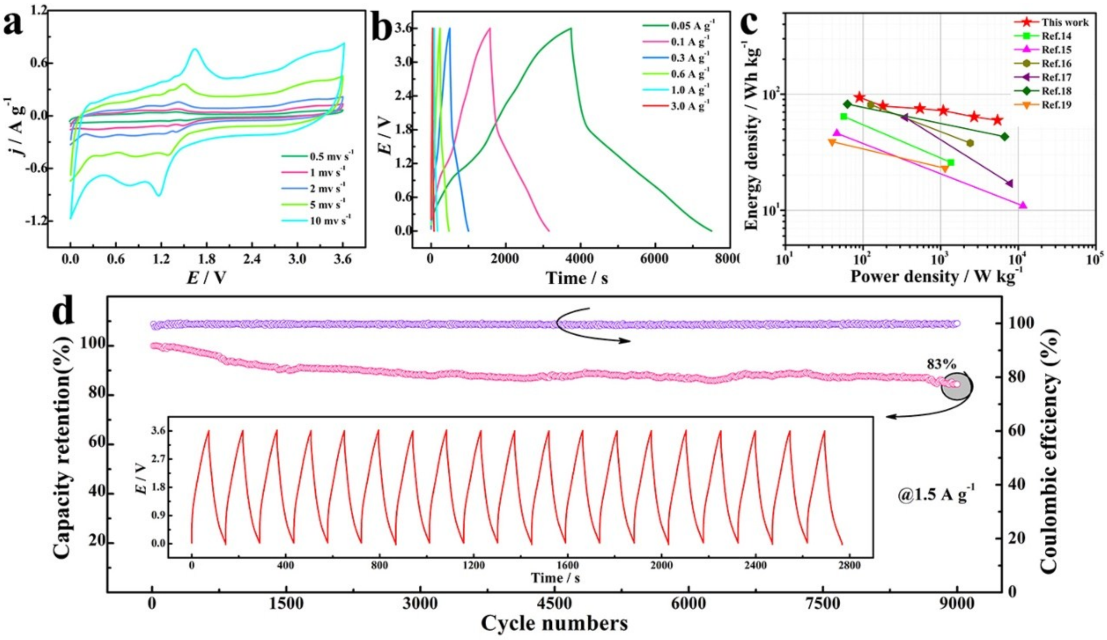

Figure S8. Electrochemical performance of MnNb$_2$O$_6$@rGO//AC SIC **(a)** CV curves at various scan rates from 0.5 to 10 mV s^{-1}; **(b)** Charge/Discharge curves at various current densities from 0.05 to 3 A g^{-1}; **(c)** Ragone plots of MnNb$_2$O$_6$@rGO//AC SIC compared with other reported SICs; **(d)** The long-term cycle life and the coulombic efficiency at 1 A g^{-1}.

Table S3. The electrochemical performance of $MnNb_2O_6$@rGO compared with other SICs reported in the literature.

Anode	Potential range	Energy density and power density	Ref.
TiO_2 Mesocages-Graphene Nanocomposite//AC	1-3.8V	64.2 Wh kg^{-1} at 56.3 W kg^{-1} 25.8 Wh kg^{-1} at 1357 W kg^{-1}	14
Titanium oxynitride mesoporous nanowires//AC	0.5-4V	46 Wh kg^{-1} at 46 W kg^{-1} 10.9 Wh kg^{-1} at 11.5 kW kg^{-1}	15
TiO_2@CNT@C//Biomass-derived Activated Carbon	1-4V	81.2 Wh kg^{-1} at 126 W kg^{-1} 37.9 Wh kg^{-1} at12.4 kW kg^{-1}	16
WS_2 nanosheets//mesoporous hollow carbon spheres	0-3.5V	63 Wh kg^{-1} at 350 W kg^{-1}; 17 Wh kg^{-1} at 7840 W kg^{-1}	17
$MoSe_2$/G//AC	0.5-3V	82 Wh kg^{-1} at 63 W kg^{-1}; 43 Wh kg^{-1} at 6688 W kg^{-1}	18
MXene//AC	0-4.0V	39 Wh kg^{-1} at ~40 W kg^{-1} 23 Wh kg^{-1} at 1140 W kg^{-1}	19
$MnNb_2O_6$@rGO//AC	0-3.6V	93.8 Wh kg^{-1} at 90 W kg^{-1}; 59.6 Wh kg^{-1} at 5400 W kg^{-1}	This work

References

1. X. Xu, Q. Zhang, Y. Yu, W. Chen, H. Hu and H. Li, *Adv. Mater.*, 2016, **28**, 9223-9230.
2. Y. H. Xie, X. X. Sheng, D. L. Xie, Z. X. Liu, X. Y. Zhang and L. Zhong, *Carbon*, 2016, **109**, 673-680.

3. S. Roldan, D. Barreda, M. Granda, R. Menendez, R. Santamaria and C. Blanco, *Phys. Chem. Chem. Phys.*, 2015, **17**, 1084-1092.
4. K. Liang, X. Tang and W. Hu, *Journal of Materials Chemistry*, 2012, **22**, 11062-11067.
5. K. Qiu, Y. Lu, D. Zhang, J. Cheng, H. Yan, J. Xu, X. Liu, J. K. Kim and Y. Luo, *Nano Energy*, 2015, **11**, 687-696.
6. L. Shen, H. Lv, S. Chen, P. Kopold, P. A. van Aken, X. Wu, J. Maier and Y. Yu, *Adv. Mater.*, 2017, **29**, 1700142.
7. H. Wang, Y. Zhang, H. Ang, Y. Zhang, H. T. Tan, Y. Zhang, Y. Guo, J. B. Franklin, X. L. Wu, M. Srinivasan, H. J. Fan and Q. Yan, *Adv. Funct. Mater.*, 2016, **26**, 3082-3093.
8. G. K. Wang, C. X. Lu, X. Zhang, B. A. Wan, H. Y. Liu, M. R. Xia, H. Y. Gou, G. Q. Xin, J. Lian and Y. G. Zhang, *Nano Energy*, 2017, **36**, 46-57.
9. M. Odziomek, F. Chaput, A. Rutkowska, K. Swierczek, D. Olszewska, M. Sitarz, F. Lerouge and S. Parola, *Nature Communications*, 2017, **8**, 1-7.
10. C.-a. Zhou, X. Xia, Y. Wang, Y. Zhong, Z. Yao, X. Wang and J. Tu, *Journal of Materials Chemistry A*, 2017, **5**, 1394-1399.
11. Y. Cai, H.-E. Wang, X. Zhao, F. Huang, C. Wang, Z. Deng, Y. Li, G. Cao and B.-L. Su, *Acs Applied Materials & Interfaces*, 2017, **9**, 10652-10663.
12. S. Li, T. Wang, W. Zhu, J. Lian, Y. Huang, Y.-Y. Yu, J. Qiu, Y. Zhao, Y.-C. Yong and H. Li, *J Mater Chem A*, 2019, **7**, 693-703.
13. X. Zhu, Q. Fu, L. Tang, C. Lin, J. Xu, G. Liang, R. Li, L. Luo and Y. Chen, *ACS*

Appl Mater Interfaces, 2018, **10**, 23711-23720.

14. Z. Le, F. Liu, P. Nie, X. Li, X. Liu, Z. Bian, G. Chen, H. B. Wu and Y. Lu, *ACS Nano*, 2017, **11**, 2952-2960.

15. J. Dong, Y. Jiang, Q. Li, Q. Wei, W. Yang, S. Tan, X. Xu, Q. An and L. Mai, *J Mater Chem A*, 2017, **5**, 10827-10835.

16. Y. E. Zhu, L. P. Yang, J. Sheng, Y. N. Chen, H. C. Gu, J. P. Wei and Z. Zhou, *Adv Energy Mater*, 2017, **7**, 9.

17. C. Ding, T. Huang, Y. Tao, D. Tan, Y. Zhang, F. Wang, F. Yu and Q. Xie, *J Mater Chem A*, 2018, **6**, 21010-21017.

18. X. Zhao, W. Cai, Y. Yang, X. Song, Z. Neale, H.-E. Wang, J. Sui and G. Cao, *Nano Energy*, 2018, **47**, 224-234.

19. N. Kurra, M. Alhabeb, K. Maleski, C.-H. Wang, H. N. Alshareef and Y. Gogotsi, *ACS Energy Letters*, 2018, **3**, 2094-2100.